

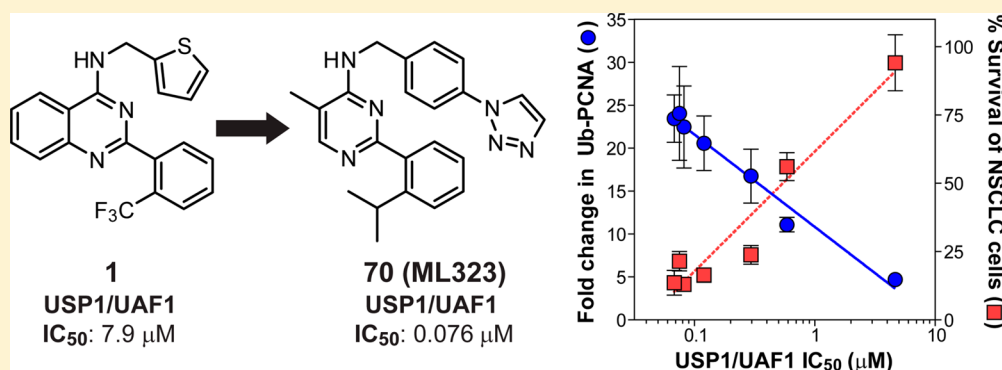
# Synthesis and Structure–Activity Relationship Studies of *N*-Benzyl-2-phenylpyrimidin-4-amine Derivatives as Potent USP1/UAF1 Deubiquitinase Inhibitors with Anticancer Activity against Nonsmall Cell Lung Cancer

Thomas S. Dexheimer,<sup>†,§</sup> Andrew S. Rosenthal,<sup>†,§</sup> Diane K. Luci,<sup>†</sup> Qin Liang,<sup>‡</sup> Mark A. Villamil,<sup>‡</sup> Junjun Chen,<sup>‡</sup> Hongmao Sun,<sup>†</sup> Edward H. Kerns,<sup>†</sup> Anton Simeonov,<sup>†</sup> Ajit Jadhav,<sup>†</sup> Zhihao Zhuang,<sup>\*,‡</sup> and David J. Maloney<sup>\*,†</sup>

<sup>†</sup>National Center for Advancing Translational Sciences, National Institutes of Health, 9800 Medical Center Drive, Rockville, Maryland 20850, United States

<sup>‡</sup>Department of Chemistry and Biochemistry, University of Delaware, 214A Drake Hall, Newark, Delaware 19716, United States

## S Supporting Information



**ABSTRACT:** Deregulation of ubiquitin conjugation or deconjugation has been implicated in the pathogenesis of many human diseases including cancer. The deubiquitinating enzyme USP1 (ubiquitin-specific protease 1), in association with UAF1 (USP1-associated factor 1), is a known regulator of DNA damage response and has been shown as a promising anticancer target. To further evaluate USP1/UAF1 as a therapeutic target, we conducted a quantitative high throughput screen of >400000 compounds and subsequent medicinal chemistry optimization of small molecules that inhibit the deubiquitinating activity of USP1/UAF1. Ultimately, these efforts led to the identification of ML323 (70) and related *N*-benzyl-2-phenylpyrimidin-4-amine derivatives, which possess nanomolar USP1/UAF1 inhibitory potency. Moreover, we demonstrate a strong correlation between compound IC<sub>50</sub> values for USP1/UAF1 inhibition and activity in nonsmall cell lung cancer cells, specifically increased monoubiquitinated PCNA (Ub-PCNA) levels and decreased cell survival. Our results establish the druggability of the USP1/UAF1 deubiquitinase complex and its potential as a molecular target for anticancer therapies.

## INTRODUCTION

Ubiquitin is a small, highly conserved protein of 76 amino acids that is post-translationally conjugated to substrate proteins, including itself, via a three-step enzymatic reaction. The initial covalent attachment primarily occurs between the C-terminal glycine of ubiquitin and the ε-amino group of lysine residue(s) of the target protein.<sup>1</sup> Additional ubiquitin molecules can be ligated to one of the seven internal lysines of ubiquitin, resulting in diverse ubiquitin chain topologies. The biological outcome of ubiquitination is determined by both the length and linkage topology.<sup>2</sup> For example, Lys48-linked polyubiquitin chains are almost exclusively associated with allocating proteins for proteasome-dependent degradation, while monoubiquitination or chains linked through different lysines have been shown

to serve multiple nonproteolytic functions.<sup>3–6</sup> Similar to other types of post-translational modifications, ubiquitination is a reversible process counter-regulated by enzymes known as deubiquitinases (DUBs), which catalyze the removal of ubiquitin from modified proteins.<sup>7</sup> More importantly, dysfunction in ubiquitin-dependent signaling pathways has been linked to various human diseases, suggesting inhibition of ubiquitin pathway components as novel therapeutic targets for drug discovery.

Pharmacological intervention within the ubiquitin–proteasome system has been well established by the successful use of

Received: July 11, 2014

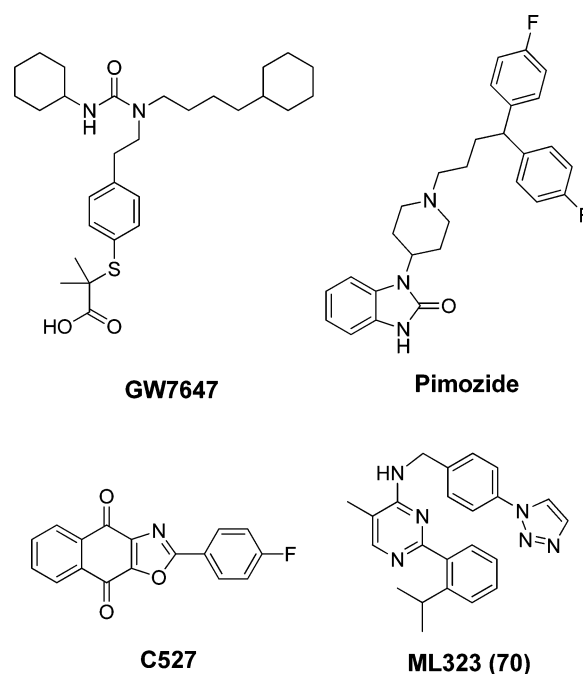
Published: September 17, 2014

proteasome inhibitors for anticancer treatment.<sup>8</sup> Nevertheless, the ubiquitin–proteasome system offers additional opportunities for therapeutic intervention that could afford increased specificity and the possibility for improved clinical efficacy, which proteasome inhibitors are currently lacking.<sup>9</sup> The most apparent targets include enzymes involved in ubiquitin conjugation and deconjugation (i.e., ubiquitin ligases and DUBs), processes upstream of proteasome-mediated protein degradation. Among the DUBs, ubiquitin-specific protease 1 (USP1) has become an attractive anticancer target because of its involvement in regulating DNA damage response pathways. USP1 associates with UAF1 (USP1-associated factor 1), resulting in the heterodimeric USP1/UAF1 complex that is required for deubiquitinase activity.<sup>10</sup> The USP1/UAF1 complex has been shown to regulate the tolerance of DNA damage induced by DNA cross-linking agents through deubiquitination of PCNA (proliferating cell nuclear antigen)<sup>11</sup> and FANCD2 (Fanconi anemia complementation group D2),<sup>12</sup> which are proteins that function in translesion synthesis and the Fanconi anemia pathway, respectively. Williams et al. also recently reported that USP1/UAF1 deubiquitinates and prevents proteasomal degradation of ID (inhibitor of DNA-binding) proteins,<sup>13</sup> which have been shown to activate multiple pathways involved in tumor progression, including preservation of the cancer stem cell phenotype.<sup>14</sup> Moreover, evidence for aberrant overexpression of USP1 in several tumor types suggests that inhibitors of USP1 are likely to provide a therapeutic benefit.<sup>13,15</sup>

Several small-molecule inhibitors of USP1/UAF1 have been identified by high-throughput screening. We initially identified the first USP1/UAF1 inhibitors, pimozone and GW7647, from a collection of bioactive molecules.<sup>16</sup> Although GW7647 and pimozone display reasonable selectivity over related proteases and demonstrate cellular inhibition of human USP1, both compounds show moderate PubChem promiscuity with a 9.5% and 11.4% hit rate, respectively, and have annotated activity against unrelated targets.<sup>17–19</sup> Since then, Mistry et al. reported C527 and related analogues, which exhibit submicromolar inhibition ( $IC_{50} = 0.88 \mu M$ ) of USP1/UAF1 activity, promote ID1 degradation, and cause cytotoxicity in several leukemic cell lines.<sup>20</sup> However, C527 displays limited selectivity for USP1/UAF1 in vitro. We recently described the discovery and biological activity of ML323 (70) (Figure 1), a novel small-molecule inhibitor of USP1/UAF1. Compound 70 was found to exhibit selective, nanomolar inhibition of USP1/UAF1 deubiquitinase activity, leading to an increase in monoubiquitinated forms of PCNA and FANCD2 and synergistic interaction with cisplatin in human tumor cell lines.<sup>21</sup> Herein, we describe the medicinal chemistry efforts that led to the selection of 70 as a chemical probe and provide biological activity and in vitro ADME data for additional analogues.

## CHEMISTRY

To initiate our medicinal chemistry efforts, we began by resynthesizing the HTS hit molecule (1), which was prepared as described in Scheme 1A/B.<sup>21</sup> The synthesis of related analogues (2–21) commenced with an EDC-mediated amide coupling between 2-aminobenzamide (i) and 2-(9-(trifluoromethyl)benzoic acid as shown in Scheme 1A.<sup>22</sup> The resulting diamide was heated to reflux with sodium hydroxide for 3 h to provide the cyclized quinazoline scaffold, which upon treatment with  $POCl_3$  gave the key intermediate 4-chloro-2-(2-(trifluoromethyl)phenyl)quinazoline (ii). This intermediate

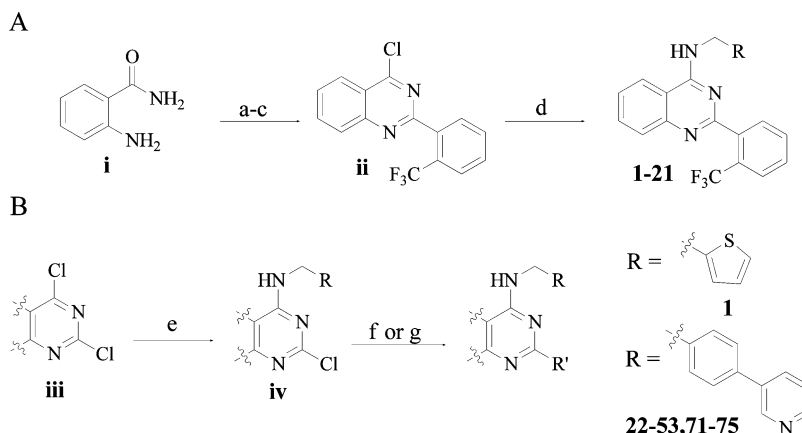


**Figure 1.** Structures of previously identified USP1/UAF1 inhibitors and ML323.

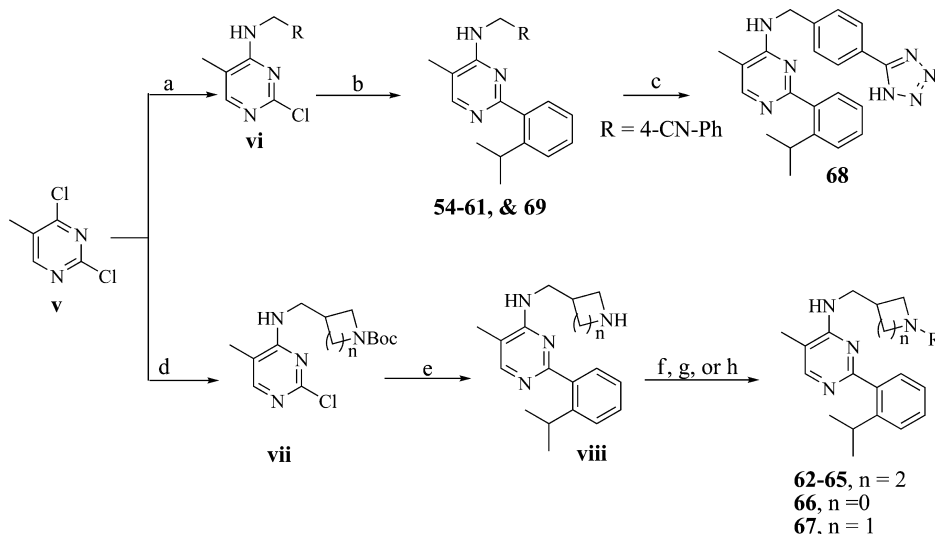
was then reacted with a variety of amines to provide analogues 2–21 (Table 1).<sup>23</sup> Notably, compound 1 could also be synthesized in this manner using thiophen-2-ylmethanamine in step d.

The synthesis of analogues 22–53 and 71–75 were all achieved in a similar manner using (4-(pyridin-3-yl)phenyl)-methanamine for the amino side chain but differed in the dichloropyrimidine-based scaffold starting material as shown in Scheme 1B. The preparation of analogues 22–36 involved addition of (4-(pyridin-3-yl)phenyl)methanamine to 2,4-dichloroquinazoline to obtain the desired chloropyrimidine intermediate (iv). Suzuki coupling of iv with various boronic acids using  $Pd(PPh_3)_4$  in a microwave reactor for 30 min at 150 °C gave analogues 22–33. For subsequent analogues, we changed to a silica bound DPP-palladium catalyst in order to alleviate any palladium contamination concerns. The synthesis of compounds 34–36 was conducted using the same sequence. However, instead of a Suzuki coupling, intermediate iv was heated in a sealed tube for 24 h at 100 °C with an excess of requisite amine. The synthetic route for compounds 37–53 (Table 3) was performed as described above starting from other commercially available 2,4-dichloropyrimidine heterocycles, and 2-isopropylphenyl boronic acid was utilized in the cross coupling reaction.

Compounds 54–69 were synthesized using 2,4-dichloro-5-methylpyrimidine (v) as the starting material along with various commercially available heterocyclic and aromatic methanamines, followed by a Suzuki coupling with 2-isopropylphenyl boronic acid (Scheme 2). The tetrazole analogue (68) was obtained via reaction of the 4-CN-Ph moiety with sodium azide in DMF. Compounds 62–67 were synthesized by reacting commercially available *tert*-butyl 4-(aminomethyl)piperidine-1-carboxylate (for 62–65), *tert*-butyl-3-(aminomethyl)pyrrolidine-1-carboxylate (for 67), or *tert*-butyl 3-(aminomethyl)azetidine-1-carboxylate (for 66), with 2,4-dichloro-5-methylpyrimidine, followed by the aforementioned Suzuki coupling conditions. The elevated temperatures used in

Scheme 1. Synthesis of Analogues 1–53 and 71–75<sup>a</sup>

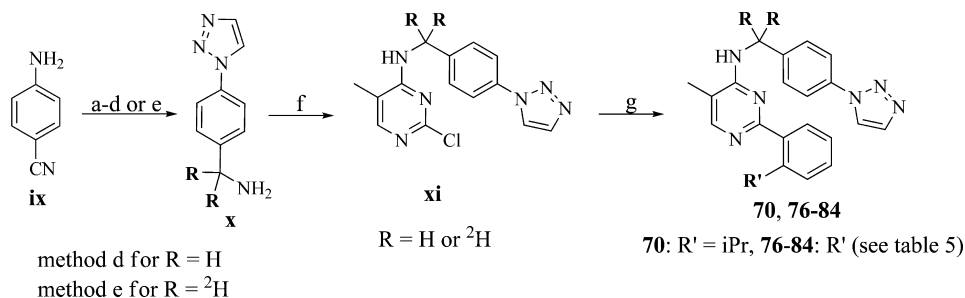
<sup>a</sup>Reagents and conditions: (a) 2-(trifluoromethyl)benzoic acid, EDC (1.2 equiv), HOBt (1.2 equiv), Et<sub>3</sub>N (3.0 equiv), CH<sub>2</sub>Cl<sub>2</sub>, 72 h; (b) 5% NaOH, reflux 3 h; (c) *N,N*-dimethylaniline, POCl<sub>3</sub>, toluene, reflux 1 h; (d) RNH<sub>2</sub>, *i*-Pr<sub>2</sub>NEt, DMF, 18 h, 60 °C; (e) for analogue **1**, [thiophen-2-ylmethanamine]; for analogues **22–53** and **71–75**, [(4-(pyridin-3-yl)phenyl)methanamine], Et<sub>3</sub>N, CHCl<sub>3</sub>, 18 h, 60 °C; (f) for analogues **22–33**, **37–53**, and **71–75**, R'B(OH)<sub>2</sub> (3 equiv), 2 M Na<sub>2</sub>CO<sub>3</sub> (4 equiv), DPP-Pd silica bound (0.3 equiv), or Pd(PPh<sub>3</sub>)<sub>4</sub> (0.2 equiv), DME, MW, 150 °C, 30–45 min; (g) for analogues **34–36**, R'NH<sub>2</sub> (3.0 equiv), THF, sealed tube 100 °C, 24 h.

Scheme 2. Synthesis of Analogues 54–69<sup>a</sup>

<sup>a</sup>Reagents and conditions: (a) 4-R-amine (1.1 equiv), Et<sub>3</sub>N (3.0 equiv), DMF, 100 °C 18 h; (b) 2-isopropylphenyl boronic acid (3.0 equiv), 2 M NaHCO<sub>3</sub> (4.0 equiv), DPP-Pd silica bound Silicycle, DME, MW, 150 °C, 30 min; (c) for R = 4-CN-Ph, NaN<sub>3</sub> (8.0 equiv), NH<sub>4</sub>Cl (8.0 equiv), DMF 130 °C, 30 min; (d) *t*-butyl 4-(aminomethyl)-R-1-carboxylate (1.1 equiv), Et<sub>3</sub>N (3.0 equiv), DMF, 100 °C 18 h; (e) 2-isopropylphenyl boronic acid (3.0 equiv), 2 M NaHCO<sub>3</sub> (4.0 equiv), DPP-Pd silica bound Silicycle, DME, MW, 150 °C, 30 min; (f) for analogues **63–64**, RBr (1.2 equiv), Cs<sub>2</sub>CO<sub>3</sub>, dicyclohexyl(2',4',6'-triisopropyl-3,6-dimethoxybiphenyl-2-yl)phosphine, RuPhos palladacycle, toluene, sealed tube, 100 °C, 18 h; (g) for analogues **65–67**, RBr (1.2 equiv), NaO<sup>t</sup>Bu, Pd<sub>2</sub>(dba)<sub>3</sub> (0.02 equiv), DavePhos (0.02 equiv) xylenes, sealed tube, 100 °C, 1 h; (h) for analogue **62**, oxetan-3-one, sodium triacetoxyborohydride (10 equiv), DCE, 2 h.

the Suzuki coupling resulted in concomitant removal of the *N*-Boc group to provide intermediates **viii**. Buchwald-Hartwig conditions for the cross coupling of the requisite amine and the heteroaryl bromides gave the desired products **63–67**.<sup>24,25</sup> Initially, we utilized the DavePhos ligand, however, this was met with limited success. Subsequent analysis of other ligands revealed that the RuPhos palladacycle proved optimal for compounds **63–64**, whereas compounds **65–67** worked best with DavePhos. Oxetan analogue (**62**) was obtained via a reductive amination of intermediate **viii** (*n* = 2) and commercially available oxetan-3-one, with sodium triacetoxyborohydride.

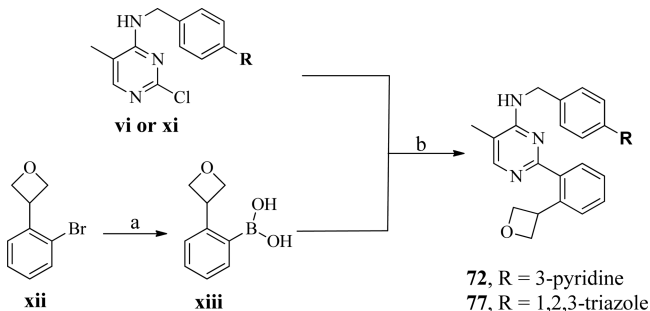
Compounds **70** (ML323, Table 4) and **76–84** (Table 5), were synthesized starting with 4-amino-benzonitrile as a TFA salt, trimethylsilyl azide, and *t*-butyl nitrite at 0 °C to give the desired azide in 98% yield (Scheme 3).<sup>26</sup> The resulting azide was dissolved in a mixture of DMSO/H<sub>2</sub>O, treated with copper sulfate, ethynyltrimethylsilane, sodium ascorbate, and heated for 24 h at 80 °C to give the desired 1,2,3-triazole. For the synthesis of the deuterated benzyl amine derivatives, we initially tried using the H-Cube flow-reactor with D<sub>2</sub>O but incomplete reduction and deuterium enrichment was observed. As such, the reduction was then carried out with lithium aluminum deuteride (LAD) to give the desired product in moderate yield (40%).<sup>27</sup> Our initial attempts for the nitrile reduction on the H-

Scheme 3. Synthesis of Analogues 70 and 76–84<sup>a</sup>

<sup>a</sup>(a) TFA (1.0 equiv), rt, 5 min then *t*-butyl nitrite (1.5 equiv), azidotrimethylsilane (1.4 equiv), 0 °C, 30 min, 98% yield; (b) ethynyltrimethylsilane (3.0 equiv), sodium ascorbate (0.8 equiv), Cu(II)SO<sub>4</sub> (0.07 equiv), DMSO/H<sub>2</sub>O (ratio 4/1) 80 °C 24 h; (c) TFA (1 equiv), acetonitrile, reflux, 1.5 h (57%); (d) H-Cube Pro, 10% Pd/C, 50 °C, 40 bar, TFA (1.2 equiv), MeOH/DMF (ratio 10/1) (98%); (e) lithium aluminum deuteride (LAD) (3.0 equiv), THF, 0 °C, 1.5 h (40%); (f) 2,4-dichloro-5-methylpyrimidine, Et<sub>3</sub>N (3 equiv), DMF, 100 °C, 18 h; (g) (2-isopropylphenyl)boronic acid (3.0 equiv), 2 M NaHCO<sub>3</sub> (4.0 equiv), DPP-Pd silica bound Silicycle, DME, 150 °C, 30 min, 35–70% yield.

Cube with a 70 mm Catcart (10% Pd/C) at 50 °C and 40 bar returned just trace amounts of product. However, the addition of TFA and changing to a MeOH/DMF mixture resulted in complete conversion to the amine (by LC-MS analysis). Given the water solubility of the 4-triazole-benzyl amine intermediates (**x**), it was used directly in the next step without further purification or characterization. The resulting mixture was heated for 18 h with 2,4-dichloro-5-methylpyrimidine and Et<sub>3</sub>N to give derivative **xi** in moderate yields of (~40%) over the two steps. Compound **xi** was then coupled to the 2-isopropylphenyl boronic acid as described previously to give the final compound **70**. Compounds **76–84** were synthesized as described above, however, several of the required boronic acids were not commercially available and had to be synthesized separately. For the deuterated analogues **80–82** and **84**, the requisite *d*<sub>6</sub> and *d*<sub>7</sub>-2-isopropylphenyl boronic acids were prepared in four steps starting from 2-bromoacetophenone (see Supporting Information for details).

The synthesis of the oxetane containing analogues **72** and **77** involved preparation of 3-(2-bromophenyl)oxetane (**xii**) using a method described by Jacobsen et al. for a comparable phenyl oxetane derivative.<sup>28</sup> Formation of the (2-(oxetan-3-yl)phenyl)-boronic acid (**xiii**) was achieved in situ via treatment of **xii** with *N*-butyllithium and triisopropyl borate in THF at –78 °C and subsequently used as-is with **vi** or **xi** to provide compounds **72** and **77**, respectively (Scheme 4).

Scheme 4. Synthesis of Analogues 72 and 77<sup>a</sup>

<sup>a</sup>(a) *N*-butyllithium (2.0 equiv), triisopropyl borate (2.0 equiv) THF, –78 °C, 18 h; (b), 2 M Na<sub>2</sub>CO<sub>3</sub> (4.0 equiv), DPP-Pd silica bound Silicycle 0.26 mmol/g (20 mol %), DME, MW, 150 °C, 30 min, 35–50% yield.

## RESULTS AND DISCUSSION

After resynthesis of the thiophene-containing HTS hit (**1**) and confirmation of its activity in both the primary Ub-rhodamine qHTS assay and orthogonal gel-based diubiquitin assay, we decided to focus our initial SAR exploration efforts around the thiophene moiety (northern portion). Despite the modest activity against USP1/UAF1 (Table 1; IC<sub>50</sub> = 7.9 μM), we were

Table 1. USP1-UAF1 Inhibition of Analogues (1–21)<sup>a</sup>

 1-11			 12-21		
Compound	R <sup>1</sup>	IC <sub>50</sub> (μM)	Compound	R <sup>2</sup>	IC <sub>50</sub> (μM)
1		7.9 ± 1.9	12		3.7 ± 1.2
2		5.1 ± 1.3	13		3.6 ± 1.5
3		3.1 ± 1.3	14		2.7 ± 1.0
4		8.4 ± 3.4	15		2.2 ± 0.6
5		6.2 ± 2.9	16		1.9 ± 0.9
6		3.4 ± 1.2	17		1.1 ± 0.4
7		4.8 ± 1.5	18		3.0 ± 1.2
8		8.9 ± 3.6	19		10.4 ± 3.8
9		10.4 ± 2.7	20		4.9 ± 1.0
10		5.7 ± 2.2	21		9.8 ± 3.4
11		8.9 ± 3.6			

<sup>a</sup>IC<sub>50</sub> values represent the half-maximal (50%) inhibitory concentration as determined in the HTS assay (*n* ≥ 3).

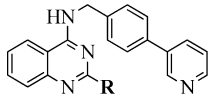
encouraged by the selectivity of this compound, with no significant activity against a small panel of DUBs and appreciable inhibition of only one of 451 kinases.<sup>21</sup> Initial changes to the thiophene functionality were generally well tolerated, with only slight changes in potency being observed. Replacing the thiophene moiety with a simple phenyl ring (**3**) led to a modest improvement in potency (3.1 μM), however, most substituted (electron-withdrawing and electron-donating



groups) phenyl rings (analogues 4–10) demonstrated fairly flat SAR. We were encouraged that substitution at the 4-position with a phenyl ring (e.g., 4-phenyl benzyl amine 12) was well tolerated with a comparable  $IC_{50}$  value of 3.7  $\mu M$ . This allowed for a variety of different analogues to be synthesized with representative examples (analogues 13–21) shown in Table 1. Potencies approached 1  $\mu M$  with both the 4-pyridine (16) and 3-pyridine (17) with  $IC_{50}$  values of 1.9 and 1.1  $\mu M$ , respectively. Given the comparable potency of these two analogues and the propensity of 4-pyridine derivatives to interact with CYPs, we decided to proceed with the 3-pyridine group for the next round of analogues which were aimed at modifying the 2- $CF_3$ -phenyl group and to investigate core scaffold changes.

Exploration of the SAR around the 2- $CF_3$ -phenyl group indicated that substitution at the 2-position was greatly favored compared to the 3- and 4-positions (Table 2). This finding is

Table 2. USP1-UAF1 Inhibition of Analogues (22–36)<sup>a</sup>



compd	R	$IC_{50}$ ( $\mu M$ )
22	3- $CF_3$ -Ph	inactive
23	4- $CF_3$ -Ph	inactive
24	2- $NO_2$ -Ph	$7.8 \pm 2.4$
25	2-OMe-Ph	$0.94 \pm 0.35$
26	2-Me-Ph	$1.1 \pm 0.4$
27	2-Et-Ph	$0.78 \pm 0.17$
28	2- <i>i</i> Pr-Ph	$0.18 \pm 0.06$
29	2-CH(F) <sub>2</sub> -Ph	$1.4 \pm 0.3$
30	2-F-Ph	$6.5 \pm 3.0$
31	2-Cl-Ph	$2.1 \pm 1.0$
32	2-Br-Ph	$1.6 \pm 0.6$
33	cyclopentyl	inactive
34	morpholine	inactive
35	pyrrolidine	inactive
36	imidazole	inactive

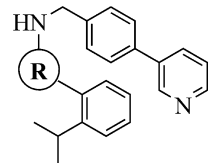
<sup>a</sup> $IC_{50}$  values represent the half maximal (50%) inhibitory concentration as determined in the HTS assay ( $n \geq 3$ ); inactive denotes an  $IC_{50} > 57 \mu M$ .

exemplified by the inactivity of the 3- $CF_3$ -phenyl (22) and 4- $CF_3$ -phenyl (23) derivatives. Given these results, we decided to focus on exploring SAR at the 2-position by replacing the  $CF_3$  group with various electron-donating/withdrawing groups as well as varying the steric bulk in this portion of the molecule. Incorporation of the electron-withdrawing group; e.g., 2- $NO_2$  (24) led to a 7-fold loss in activity, whereas the electron-donating group, e.g., 2-OMe (25), provided comparable activity ( $IC_{50} = 0.94 \mu M$ ). Replacement with the simple alkyl substituents (R = 2-Me, 26 or R = 2-Et, 27) also provided comparable activity to the 2- $CF_3$  group. Our biggest potency improvement (6-fold) occurred when we replaced the 2- $CF_3$  with an isopropyl group (28), which had an  $IC_{50}$  of 180 nM. Changing the methyl groups of the isopropyl moiety to fluoro groups (29) led to an appreciable decrease in potency. Other electron-withdrawing groups were prepared (analogues 30–32), yet none of these had improved activity. Finally, modification of the phenyl ring to a cyclopentyl group (33) or nitrogen containing heterocycles (34–36) resulted in inactive compounds. Having already improved the potency

over the original HTS hit compound 1 from 4.7 to 0.18  $\mu M$  (26-fold), we decided to turn our attention toward modification of the quinazoline core.

Initial data from analogues in our qHTS collection suggested that replacement of the quinazoline core with a pyrimidine would be tolerated. This change would be beneficial in that it would reduce the molecular weight and lipophilicity of the lead compound. Gratifyingly, this modification was in fact tolerated and resulted in a compound with comparable potency (37, Table 3). Introduction of a 5-methyl group (38) resulted in a

Table 3. USP1-UAF1 Inhibition of Analogues (37–53)<sup>a</sup>



Compound	R	$IC_{50}$ ( $\mu M$ )	Compound	R	$IC_{50}$ ( $\mu M$ )
37		$0.15 \pm 0.04$	45		$0.16 \pm 0.04$
38		$0.07 \pm 0.03$	46		$0.11 \pm 0.03$
39		$0.21 \pm 0.04$	47		$0.28 \pm 0.05$
40		$0.12 \pm 0.05$	48		$0.08 \pm 0.02$
41		$0.12 \pm 0.03$	49		$0.07 \pm 0.02$
42		$2.9 \pm 1.1$	50		$0.11 \pm 0.05$
43		$0.26 \pm 0.07$	51		$0.31 \pm 0.06$
44		$0.86 \pm 0.23$	52		$0.19 \pm 0.05$
			53		$0.11 \pm 0.03$

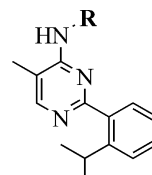
<sup>a</sup> $IC_{50}$  values represent the half-maximal (50%) inhibitory concentration as determined in the HTS assay ( $n \geq 3$ ).

~2-fold increase in potency with an  $IC_{50}$  value of 70 nM. Interestingly, moving the methyl group to the 6-position (39) resulted in a 3-fold decrease in potency (210 nM). The 5,6-dimethyl derivative (40) was also well tolerated as was the cyclopentylpyrimidine analogue 45, with  $IC_{50}$  values of 120 and 160 nM, respectively. Incorporation of other heteroaromatic core scaffolds (41–44 and 46–48) provided compounds with good potency, with the most potent being the furan derivative 48. Other groups such as OMe (49), F (50),  $NH_2$  (51),  $NMe_2$  (52), and SMe (53) provided good potency with  $IC_{50}$  values of 70, 110, 310, 190, and 110 nM, respectively. However, as stated above, our interest in these structural modifications was to improve or maintain potency while reducing molecular weight. Therefore, we decided to continue our SAR explorations with the 5-methyl-pyrimidine (38) as the core scaffold given the potent inhibition (70 nM) and reduced size.

Having established the 5-methyl pyrimidine core and the 2-isopropyl group as optimal, we then decided to return to exploration of the “northern portion” SAR. Despite the potency of the terminal 3-pyridine group, some initial ADME data suggested that this group may be a metabolic liability.

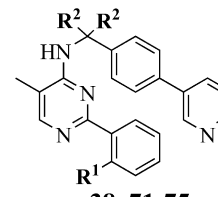
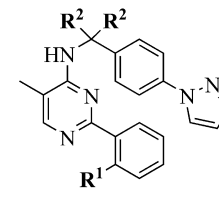
Replacement of the 4-(3-pyridine)-benzyl amine with a simple 3-methyl-phenyl (**54**), 3-pyridine (**55**), or thiophene (**56**) generally showed good potency in the Ub-Rho assay (130, 1300, and 270 nM, respectively), however, none of these had comparable potency to **38** in the orthogonal diubiquitin assay (data not shown). In an attempt to increase the hydrophilicity of the compound, a branched hydroxymethyl group (**57**) was introduced; however, this led to a large decrease in potency. Replacement of the phenyl group with an N-Me-piperidine (**58**) led to complete loss of activity. Given these data, we returned our focus to the two ring analogues (**59–70**). Adding a fluoro (**59**) or methyl (**60**) group,  $\alpha$  to the pyridine nitrogen, was well tolerated (**59**,  $IC_{50}$  = 80 nM; **60**,  $IC_{50}$  = 50 nM), which could help alleviate potential CYP interactions if necessary. However, these changes increase lipophilicity, which is something we were trying to avoid if possible. Looking to increase the  $sp^3$  character of this side chain, we replaced the central phenyl group with a piperidine (analogues **62–65**), which generally resulted in comparable potency with exception of oxetane derivative **62**. However, the corresponding four-membered (**66**) and five-membered (**67**) rings resulted in a loss of potency with  $IC_{50}$  values of 21.7 and 0.8  $\mu$ M, respectively. These data seem to indicate a size preference for six-membered ring with the potency rank order being phenyl  $\approx$  piperidine > pyrrolidine  $\gg$  azetidine. In an attempt to attenuate the potential metabolic liability of the 3-pyridine moiety, several other nitrogen containing heterocycles were prepared and tested (analogues **68–70**). The imidazole derivative (**69**) demonstrated moderate potency (300 nM), whereas the tetrazole (**68**) resulted in a significant decrease in potency. The latter result is unsurprising given the  $pK_a$  differences in these heterocycles and the general preference for basic moieties in this position (e.g., pyridine). However, we were particularly intrigued by the 1,2,3-triazole derivative (**70**,  $IC_{50}$  = 76 nM), given its improved metabolic stability, cell permeability, and activity in other biological assays (vide infra).<sup>21</sup>

Compound **70** demonstrated modest metabolic stability ( $T_{1/2}$  = 15 min) as shown in Table 5, and Met ID studies (see Supporting Information, Figure S1) indicated that the two major metabolites involving oxidative removal of the *N*-benzyl group and hydroxylation of the isopropyl group. As such, in an effort to improve the half-life we first focused on the benzylic position and synthesized *gem*-dimethyl analogues **79** and **82** and deuterated analogues **83** and **84**. Direct hydrogen abstraction is thought to be the rate-limiting step for CYP-mediated hydroxylation of aliphatic compounds, and C–H bond cleavage is approximately 6–10 times faster than the corresponding C–D bond (kinetic isotope effect).<sup>29,30</sup> Thus, replacement of metabolically labile hydrogen atoms with deuterium has been an attractive concept in drug discovery, as the change should have a negligible effect on the physicochemical properties yet improve metabolic stability.<sup>10</sup> Accordingly, we sought to utilize this strategy at both the benzylic position and 2-isopropyl moiety in effort to obviate metabolic instability. We thought this approach was particularly attractive for the 2-isopropyl group because our SAR efforts revealed this to be critical for activity and not easily replaced. Unfortunately, despite thorough investigation of various deuterated analogues (**80–84**), we did not notice any appreciable improvement in the metabolic half-life of this series. Analogue **79**, which possesses the *gem*-dimethyl group, did show a moderate improvement in our studies, however, it remained below the desired stability of >30 min. In an attempt

Table 4. USP1-UAF1 Inhibition of Analogues (**54–70**)<sup>a</sup>


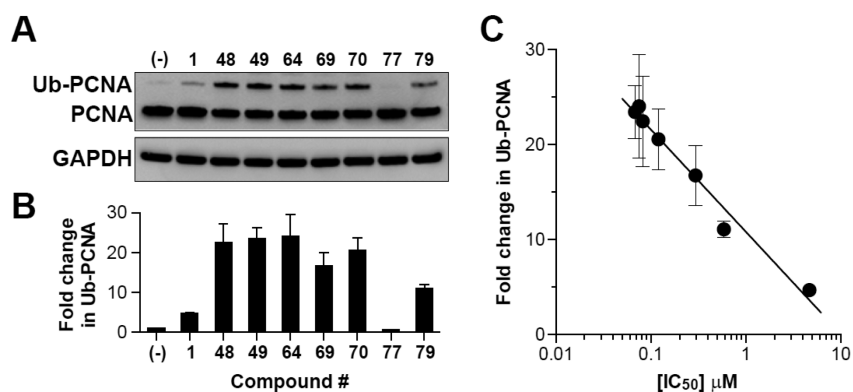
Compound	R	$IC_{50}$ ( $\mu$ M)	Compound	R	$IC_{50}$ ( $\mu$ M)
<b>54</b>		$0.13 \pm 0.04$	<b>63</b>		$0.14 \pm 0.04$
<b>55</b>		$1.3 \pm 0.3$	<b>64</b>		$0.08 \pm 0.04$
<b>56</b>		$0.27 \pm 0.07$	<b>65</b>		$0.09 \pm 0.03$
<b>57</b>		$21 \pm 3.6$	<b>66</b>		$21.7 \pm 8.6$
<b>58</b>		inactive	<b>67</b>		$0.8 \pm 0.3$
<b>59</b>		$0.08 \pm 0.04$	<b>68</b>		$5.9 \pm 1.7$
<b>60</b>		$0.05 \pm 0.01$	<b>69</b>		$0.30 \pm 0.14$
<b>61</b>		$0.32 \pm 0.08$	<b>70</b>		$0.076 \pm 0.014$
<b>62</b>		$13.6 \pm 2.1$			

<sup>a</sup> $IC_{50}$  values represent the half-maximal (50%) inhibitory concentration as determined in the HTS assay ( $n \geq 3$ ); inactive denotes an  $IC_{50} > 57 \mu$ M.

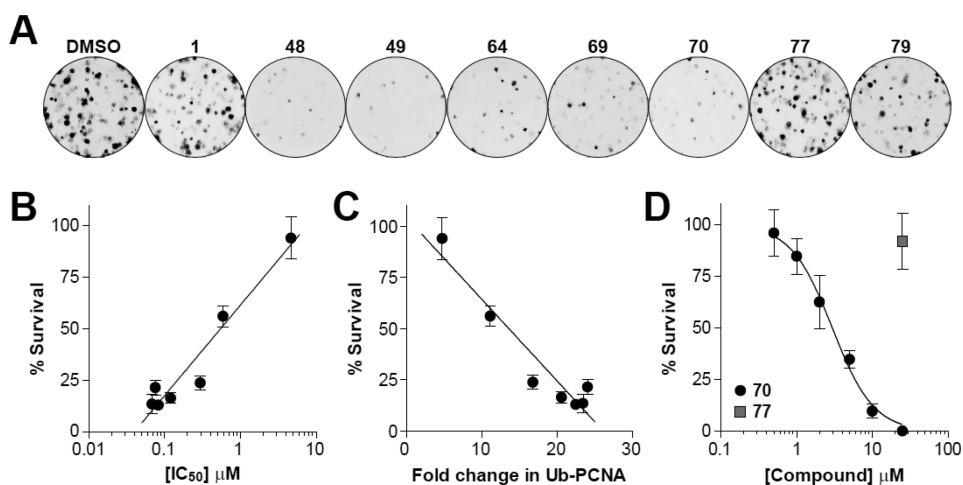
Table 5. USP1-UAF1 Inhibition of Analogues (**38**, **70–84**)<sup>a</sup>



compd	R <sup>1</sup>	R <sup>2</sup>	$IC_{50}$ ( $\mu$ M)	$T_{1/2}$ (min) <sup>b</sup>
<b>38</b>	CH(CH <sub>3</sub> ) <sub>2</sub>	H	$0.07 \pm 0.03$	5.8
<b>71</b>	cyclopropane	H	$0.18 \pm 0.07$	6.2
<b>72</b>	oxetane	H	inactive	>30
<b>73</b>	CH <sub>2</sub> OH	H	$10.5 \pm 1.9$	ND
<b>74</b>	CH(OH)CH <sub>3</sub>	H	$2.0 \pm 0.8$	ND
<b>75</b>	C(O)CH <sub>3</sub>	H	$8.7 \pm 2.1$	ND
<b>70</b>	CH(CH <sub>3</sub> ) <sub>2</sub>	H	$0.076 \pm 0.014$	15
<b>76</b>	cyclobutane	H	$0.18 \pm 0.09$	5.1
<b>77</b>	oxetane	H	inactive	>30
<b>78</b>	CHF <sub>2</sub>	H	$0.82 \pm 0.25$	21
<b>79</b>	CH(CH <sub>3</sub> ) <sub>2</sub>	CH <sub>3</sub>	$0.59 \pm 0.12$	22
<b>80</b>	CH(CD <sub>3</sub> ) <sub>2</sub>	H	$0.14 \pm 0.04$	7.9
<b>81</b>	CD(CD <sub>3</sub> ) <sub>2</sub>	H	$0.10 \pm 0.04$	9.5
<b>82</b>	CD(CD <sub>3</sub> ) <sub>2</sub>	CH <sub>3</sub>	$0.76 \pm 0.14$	10
<b>83</b>	CH(CH <sub>3</sub> ) <sub>2</sub>	D	$0.12 \pm 0.05$	12
<b>84</b>	CD(CD <sub>3</sub> ) <sub>2</sub>	D	$0.19 \pm 0.04$	13

<sup>a</sup> $IC_{50}$  values represent the half-maximal (50%) inhibitory concentration as determined in the HTS assay ( $n \geq 3$ ); inactive denotes an  $IC_{50} > 57 \mu$ M. <sup>b</sup>Represents the half-life in minutes of the compounds in the presence of rat liver microsomes (with NADPH).



**Figure 2.** Disruption of USP1/UAF1-catalyzed deubiquitination of PCNA in H1299 cells. (A) H1299 cells were treated with the indicated compounds at  $20 \mu\text{M}$  for 4 h. Whole cell extracts were separated on 4–12% gradient SDS-PAGE and subjected to Western blotting with antibodies against PCNA and GAPDH (loading control). (B) Fold changes in monoubiquitinated PCNA (Ub-PCNA) were calculated by normalizing to unmodified PCNA and GAPDH. The data represent the mean  $\pm$  SEM of two biological replicates. (C) Correlation between mean  $IC_{50}$  values obtained in the HTS assay and fold change in Ub-PCNA in H1299 cells (Pearson  $r = -0.988$ ;  $P < 0.0001$ ).



**Figure 3.** Effects of USP1/UAF1 inhibition on cell survival in H1299 cells. (A) Representative colony formation assays (CFA) in H1299 cells after treatment with indicated compounds. Cells were grown in the absence or presence of  $5 \mu\text{M}$  of compound for 7 days and stained with crystal violet. (B) Correlation between mean  $IC_{50}$  values obtained in the HTS assay and percent survival at  $5 \mu\text{M}$  in H1299 cells (Pearson  $r = 0.967$ ;  $P = 0.0004$ ). (C) Correlation between fold change in Ub-PCNA (see Figure 2A,B) and percent survival at  $5 \mu\text{M}$  in H1299 cells (Pearson  $r = -0.954$ ;  $P = 0.0008$ ). (D) Survival curve using CFA in H1299 cells treated with increasing concentrations of 70 or  $25 \mu\text{M}$  of 77.

to address the undesired aliphatic hydroxylation at isopropyl group, we synthesized the cyclopropyl (71), cyclobutyl (76), oxetane (72 and 77), and difluoro (78) derivatives. While the cyclopropyl (71) and cyclobutyl (76) analogues demonstrated potent inhibition ( $IC_{50} = 180 \text{ nM}$ ), the metabolic stability was not improved, with  $T_{1/2} = 6.2$  and  $5.1 \text{ min}$ , respectively. Replacement of lipophilic moieties with an oxetane group has been shown to improve the metabolic stability and solubility of the parent compound.<sup>31</sup> Interestingly, this result was realized in our case, as both oxetane derivatives (72 and 77) had favorable metabolic stability ( $T_{1/2} > 30 \text{ min}$ ) and solubility (data not shown), however, they had lost all activity toward USP1/UAF1. While disappointed by this result, we decided to use compound 77 as our inactive control in subsequent biological studies, making it a vital analogue. The preference for having lipophilic moieties at the 2-position of the phenyl ring was further solidified with the testing of the alcohol (73–74) and ketone (75) analogues, which exhibited potencies in the micromolar range.

Our detailed SAR explorations around compound 1 led to a sufficient understanding of the structural features that are

required for USP1/UAF1 inhibition. Thus, we sought to further evaluate the cellular activity of a number of selected compounds. We initially assessed the ability of the compounds to modulate USP1/UAF1 activity in cells by monitoring the level of monoubiquitinated PCNA (Ub-PCNA). Upon treatment of H1299 nonsmall cell lung cancer cells with select compounds (1, 64, 70, and 77), we observed a dose-dependent increase in Ub-PCNA compared to both the untreated control and the inactive oxetane analogue (77) (see Supporting Information, Figure S2). Importantly, an increase in Ub-PCNA was observed at concentrations as low as  $1 \mu\text{M}$  for top compounds (e.g., 64 and 70). To ensure that a robust increase in Ub-PCNA was observed, additional compounds were tested at a fixed concentration of  $20 \mu\text{M}$ . As shown in Figure 2A,B, several compounds significantly increased the level of Ub-PCNA. More importantly, we observed a linear correlation between the logarithm of  $IC_{50}$  values obtained in the HTS assay and fold change in Ub-PCNA ( $R^2 = 0.98$ , Figure 2C). In addition to validating the reliability of the HTS assay, these results further support the on-target effects of this compound



Table 6. In vitro ADME Profile<sup>a</sup>

compd	PBS buffer (pH 7.4) solubility ( $\mu$ M)	Log <i>D</i> (pH 7.4)	microsomal stability ( $T_{1/2}$ in min)			Caco-2 (A→B) $P_{app}$ ( $10^{-6}$ cm/s)	efflux ratio	PBS buffer (pH 7.4) stability (48 h) (%)	mouse plasma stability (2 h) (%)
70	86	1.97	15 RLM	26 HLM	15 MLM	22.98	0.9	99	99

<sup>a</sup>Aqueous solubility (PBS buffer), mouse liver microsome (MLM) human liver microsome stability (HLM), Caco-2, and plasma stability studies were conducted at Pharmaron Inc. The Log *D* data was conducted by Analiza Inc. using a miniaturized shake-flask methodology. The rat liver microsome (RLM) studies were conducted at NCATS. The microsomal stability data represents the stability in the presence of NADPH. Compound 70 showed no degradation without NADPH present over a 1 h period.

series in preventing the USP1/UAF1-catalyzed deubiquitination of PCNA in human cells.<sup>21</sup>

We next examined the effects of these compounds on cell survival using a colony formation assay. As shown in Figure 3A, several of the compounds markedly inhibited the colony-forming capacity of H1299 cells relative to DMSO-treated control. Five compounds (48, 49, 64, 69, and 70) caused greater than 70% reduction of colony formation at 5  $\mu$ M, whereas the original HTS hit (1) and the inactive oxetane analogue (77) had minimal or no effect on cell survival, respectively. A direct correlation between IC<sub>50</sub> values for USP1/UAF1 inhibition and cell survival was identified ( $R^2$  = 0.93, Figure 3B). As anticipated, the fold change in Ub-PCNA also correlated with cell survival ( $R^2$  = 0.91, Figure 3C), suggesting PCNA monoubiquitination as a candidate pharmacodynamic biomarker predictive of efficacy. Compound 70 was further evaluated in dose–response and demonstrated to have an EC<sub>50</sub> of 3.0  $\mu$ M, while the inactive analogue 77 had no effect on cell survival up to 25  $\mu$ M (Figure 3D). These results suggest that USP1/UAF1 inhibitors could show promise as a monotherapy despite being initially envisioned as a combination therapy with DNA damaging agents.<sup>16,21,32</sup>

**In Vitro ADME Profile.** Having already evaluated the selectivity of this molecule against numerous DUBs, human proteases, and kinases,<sup>21</sup> we next wanted to determine ancillary pharmacology against GPCR and ion channel and transporter targets. To do so, we tested compound 70 at 10  $\mu$ M in the CEREP LeadProfilingScreen2, which contains 80 different GRCRs, ion channels, and transporters. Once again, compound 70 demonstrated an encouraging selectivity profile, with only 7 targets showing inhibition of >50% at 10  $\mu$ M (5-HT<sub>2A/2B/2C</sub>, A<sub>3</sub>, Ca<sup>2+</sup> channel, MT<sub>1</sub>, and PPAR $\gamma$ ) (see Supporting Information, Figure S4). A selection of the in vitro ADME attributes of compound 70 is highlighted in Table 6. Notably, compound 70 possesses good kinetic solubility in PBS buffer (pH 7.4) of 86  $\mu$ M, and the experimental Log *D* (pH 7.4) of 1.97 is well within the ideal range for orally bioavailable drug-like molecules. This value was obtained by Analiza Inc. using their “scaled-down shake flask lipophilicity” method. As anticipated, compound 70 is stable in PBS buffer, assay buffer, pH 2, pH 9 (see Supporting Information, Figure S3, and mouse plasma (Table 6). Compound 70 also exhibits excellent Caco-2 permeability [ $P_{app}$  = 23 ( $10^{-6}$  cm/s)] and shows no signs of efflux (ratio = 0.9), which seems to indicate the compound is not subject to the action of transporters, such as Pgp. One remaining liability is the less than optimal microsomal stability, with an observed  $T_{1/2}$  of 15 min (rat and mouse liver microsomes) and 26 min (human liver microsome). While our efforts to improve this liability have thus far been met with limited success, we fully expect that through further medicinal chemistry optimization this metabolic liability can be attenuated. Finally, preliminary in vivo PK studies of this compound indicate favorable bioavailability (>80%) yet rapid clearance (>70 mL/min/kg),

which is likely a result of the marginal phase I metabolic stability discussed above.

## CONCLUSION

DUBs have been implicated in cancer and other human diseases and thus have become increasingly regarded as prospective targets for therapeutic intervention.<sup>33–35</sup> Here, we summarize the medicinal chemistry optimization efforts of a series of *N*-benzyl-2-phenylpyrimidin-4-amine based USP1/UAF1 deubiquitinase inhibitors. We succeeded in generating several inhibitors with nanomolar potency, which corresponds to  $\geq 100$ -fold improved activity compared to the original HTS hit (1). In addition, we demonstrate activity in cells with selected compounds as single agents, specifically increasing the level of monoubiquitinated-PCNA and decreasing cell survival in nonsmall cell lung cancer cells (Figure 2 and 3). It has recently been demonstrated that small-molecule inhibitors of USP1/UAF1 are cytotoxic to both established leukemic cell lines and patient-derived leukemic cells.<sup>20</sup> The data presented here also supports the use of USP1/UAF1 inhibitors as a monotherapy in nonsmall cell lung cancer (Figure 3). In addition to further medicinal chemistry optimization to improve ADME properties, we are currently attempting to identify cancer subtypes or patient populations that may benefit from USP1/UAF1-targeted therapy.

## EXPERIMENTAL SECTION

**General Chemistry Methods.** All air or moisture sensitive reactions were performed under positive pressure of nitrogen with oven-dried glassware. Chemical reagents and anhydrous solvents were obtained from commercial sources and used as-is. Preparative purification was performed on a Waters semipreparative HPLC. The column used was a Phenomenex Luna C18 (5  $\mu$ m, 30 mm  $\times$  75 mm) at a flow rate of 45 mL/min. The mobile phase consisted of acetonitrile and water (each containing 0.1% trifluoroacetic acid). A gradient of 10–50% acetonitrile over 8 min was used during the purification. Fraction collection was triggered by UV detection (220 nm). Analytical analysis for purity was determined by two different methods denoted as final QC methods 1 and 2. Method 1: Analysis was performed on an Agilent 1290 Infinity series HPLC UHPLC long gradient equivalent 4–100% acetonitrile (0.05% trifluoroacetic acid) in water over 3.5 min run time of 4 min with a flow rate of 0.8 mL/min. A Phenomenex Kinetex 1.7  $\mu$ m C18 column (2.1 mm  $\times$  100 mm) was used at a temperature of 50  $^{\circ}$ C. Method 2: Analysis was performed on an Agilent 1260 with a 7 min gradient of 4–100% acetonitrile (containing 0.025% trifluoroacetic acid) in water (containing 0.05% trifluoroacetic acid) over 8 min run time at a flow rate of 1 mL/min. A Phenomenex Luna C18 column (3  $\mu$ m, 3 mm  $\times$  75 mm) was used at a temperature of 50  $^{\circ}$ C. Purity determination was performed using an Agilent diode array detector for both method 1 and method 2. Mass determination was performed using an Agilent 6130 mass spectrometer with electrospray ionization in the positive mode. All of the analogues for assay have purity greater than 95% based on both analytical methods. <sup>1</sup>H and <sup>13</sup>C NMR spectra were recorded on a Varian 400 (100) MHz spectrometer. High resolution mass



spectrometry was recorded on Agilent 6210 time-of-flight LC-MS system.

*N*-(Thiophen-2-ylmethyl)-2-(2-(trifluoromethyl)phenyl)-quinazolin-4-amine (**1**).<sup>21</sup> 2,4-Dichloroquinazoline (0.50 g, 2.51 mmol), thiophen-2-ylmethanamine (0.34 g, 3.0 mmol), and triethylamine (Et<sub>3</sub>N) (1.0 mL, 7.54 mmol) was stirred overnight in CH<sub>2</sub>Cl<sub>2</sub> (6.0 mL) at room temperature. The reaction mixture was poured into water and extracted (3×) with CH<sub>2</sub>Cl<sub>2</sub>, and the organic layers were combined, washed (1×) with brine, dried over Na<sub>2</sub>SO<sub>4</sub>, filtered, and concentrated to provide 2-chloro-*N*-(thiophen-2-ylmethyl)quinazolin-4-amine, which was used without further purification in the next reaction. LC-MS retention time (method 1) = 3.334 min.

A 5 mL microwave reaction vessel was charged with a mixture of the above-mentioned 2-chloro-*N*-(thiophen-2-ylmethyl)quinazolin-4-amine (0.09 g, 0.31 mmol), 2-(trifluoromethyl)phenylboronic acid (0.18 g, 0.96 mmol), Pd(PPh<sub>3</sub>)<sub>4</sub> (0.06 g, 0.05 mmol), sodium carbonate (0.40 M in water, 1.2 mL, 0.48 mmol), and acetonitrile (1.2 mL). The vessel was sealed and heated, with stirring, at 150 °C for 10 min via microwave irradiation. The organic portion was concentrated under reduced pressure, and the residue was purified by silica gel chromatography using (80% hexanes, 20% ethyl acetate) to give the desired product. <sup>1</sup>H NMR (400 MHz, DMSO-*d*<sub>6</sub>) δ 8.47–8.37 (m, 1 H), 8.03–7.75 (m, 7 H), 7.71 (ddd, *J* = 1.25, 7.10, and 8.34 Hz, 1 H), 7.38 (dd, *J* = 1.27, and 5.12 Hz, 1 H), 7.07 (dd, *J* = 1.22, and 3.43 Hz, 1 H), 6.95 (dd, *J* = 3.46, and 5.09 Hz, 1 H) and 5.03 (d, *J* = 5.70 Hz, 2 H). <sup>13</sup>C NMR (101 MHz, DMSO-*d*<sub>6</sub>) δ 160.09, 159.72, 158.66, 158.33, 140.73, 135.43, 132.43, 131.94, 130.96, 128.01, 127.70, 127.40, 126.24, 125.67, 123.93, 122.95, 118.24, 115.30, 112.89, and 40.60. LC-MS retention time (method 2) = 4.808 min and (method 1) = 3.128 min. HRMS: *m/z* (M + H)<sup>+</sup> (calculated for C<sub>20</sub>H<sub>15</sub>F<sub>3</sub>N<sub>3</sub>S 386.0933) found, 386.0942.

2-(2-Isopropylphenyl)-*N*-(4-(pyridin-3-yl)benzyl)furo[3,2-*d*]pyrimidin-4-amine (**48**). 2,4-Dichlorofuro[3,2-*d*]pyrimidine (0.10 g, 0.53 mmol), (4-(pyridin-3-yl)phenyl)methanamine (0.10 g, 0.53 mmol), and triethylamine (0.22 mL, 1.59 mmol) were heated in chloroform to 50 °C for 18 h. The mixture was poured into saturated NaHCO<sub>3</sub> and extracted with chloroform (2×). The organic layers were combined, dried over Na<sub>2</sub>SO<sub>4</sub>, filtered, and concentrated to give an oil which was used in the next step without further purification. LC-MS retention time (method 1) = 2.692 min. 2-Chloro-*N*-(4-(pyridin-3-yl)benzyl)furo[3,2-*d*]pyrimidin-4-amine (72 mg, 0.21 mmol), (2-isopropylphenyl)boronic acid (42 mg, 0.26 mmol), Pd(PPh<sub>3</sub>)<sub>4</sub> (25 mg, 0.02 mmol), and sodium carbonate (2 M, 0.21 mL, 0.43 mmol) in 1,2-dimethoxyethane (2 mL) was sealed in a microwave tube and heated to 150 °C for 30 min in a Biotage microwave reactor. The reaction was filtered through a pad of Celite and washed with ethyl acetate, concentrated, and purified on reversed phase to give the desired compound. <sup>1</sup>H NMR (400 MHz, DMSO-*d*<sub>6</sub>) δ 9.46 (br s, 1 H), 8.95 (d, *J* = 1.96 Hz, 1 H), 8.63 (d, *J* = 5.09 Hz, 1 H), 8.47 (s, 1 H), 8.23 (d, *J* = 7.83 Hz, 1 H), 7.73 (d, *J* = 8.22 Hz, 2 H), 7.62 (dd, *J* = 5.09, and 7.83 Hz, 1 H), 7.40–7.53 (m, 5 H), 7.24–7.33 (m, 1 H), 7.12 (d, *J* = 1.96 Hz, 1 H), 4.86 (d, *J* = 5.87 Hz, 2 H), 3.31 (ddd, *J* = 6.85, 7.04, and 13.50 Hz, 1 H), 1.05 (s, 3 H), and 1.03 (s, 3 H). LC-MS retention time (method 1): 2.706 min; (method 2): 4.214 min. HRMS: *m/z* (M + H)<sup>+</sup> (calculated for C<sub>27</sub>H<sub>26</sub>N<sub>4</sub>O 421.2023) found, 421.2011.

2-(2-Isopropylphenyl)-5-methoxy-*N*-(4-(pyridin-3-yl)benzyl)pyrimidin-4-amine (**49**). Follow the synthesis for compound **48** and substitute 2,4-dichloro-5-methoxypyrimidine for 2,4-dichlorofuro[3,2-*d*]pyrimidine to give the desired product. <sup>1</sup>H NMR (400 MHz, DMSO-*d*<sub>6</sub>) δ 9.51–9.67 (m, 1 H), 8.88–8.97 (m, 1 H), 8.63 (d, *J* = 4.70 Hz, 1 H), 8.16–8.25 (m, 1 H), 8.11 (s, 1 H), 7.71 (d, *J* = 8.22 Hz, 2 H), 7.32–7.64 (m, 7 H), 4.78 (d, *J* = 5.87 Hz, 2 H), 3.97–4.08 (m, 3 H), 2.98–3.10 (tddd, *J* = 6.46, 6.60, 6.73, and 13.52 Hz, 1 H), 1.02 (s, 3 H), and 1.01 (s, 3 H). <sup>13</sup>C NMR (151 MHz, DMSO-*d*<sub>6</sub>) δ 155.72, 155.29, 147.79, 146.91, 146.03, 139.07, 138.69, 136.71, 136.44, 135.48, 131.79, 131.63, 129.87, 128.21, 127.46, 126.66, 126.22, 125.19, 57.72, 43.90, 29.42, and 24.12. LC-MS retention time (method 1), 2.738 min; (method 2), 1.489 min. HRMS: *m/z* (M + H)<sup>+</sup> (calculated for C<sub>26</sub>H<sub>27</sub>N<sub>4</sub>O 411.2179) found, 411.2181.

2-(2-Isopropylphenyl)-5-methyl-*N*-((1-(pyridin-3-yl)piperidin-4-yl)methyl)pyrimidin-4-amine (**64**). The synthetic method for compound **48** was followed and 2,4-dichloro-5-methylpyrimidine was substituted for 2,4-dichlorofuro[3,2-*d*]pyrimidine and *tert*-butyl 4-(aminomethyl)piperidine-1-carboxylate for (4-(pyridin-3-yl)phenyl)methanamine to give the desired product. The cross coupling step removed the *tert*-butyl carbamate to give 2-(2-isopropylphenyl)-5-methyl-*N*-(piperidin-4-ylmethyl)pyrimidin-4-amine, which was purified on silica gel with CH<sub>2</sub>Cl<sub>2</sub>/MeOH (saturated with NH<sub>3</sub>). LC-MS retention time (method 1): 2.538 min. This compound was used in the next step with no further characterization. To degassed xylene (5 mL), 2-(2-isopropylphenyl)-5-methyl-*N*-(piperidin-4-ylmethyl)pyrimidin-4-amine (0.52 g, 1.60 mmol), 2'-(dicyclohexylphosphino)-*N,N*-dimethylbiphenyl-2-amine (DavePhos) (0.01 g, 0.02 mmol), sodium *tert*-butoxide (0.22 g, 1.4 mmol), Pd<sub>2</sub>(dba)<sub>3</sub> (0.02g, 0.02 mmol), and 3-bromopyridine (0.30 g, 1.92 mmol) were added and heated in a sealed tube to 100 °C for 18 h. The reaction material was loaded directly onto silica gel and purified using (0–10% MeOH/DCM). <sup>1</sup>H NMR (400 MHz, DMSO-*d*<sub>6</sub>) δ 8.67–8.79 (m, 1 H), 8.37 (d, *J* = 2.74 Hz, 1 H), 8.23 (s, 1 H), 8.08 (d, *J* = 5.09 Hz, 1 H), 7.72–7.83 (m, 1 H), 7.53–7.62 (m, 3 H), 7.45–7.52 (m, 1 H), 7.34–7.43 (m, 1 H), 3.81–3.94 (m, 2 H), 3.19–3.28 (m, 1 H), 2.80 (t, *J* = 11.74 Hz, 2 H), 2.18 (s, 3 H), 1.89 (dd, *J* = 3.72, and 7.14 Hz, 1 H), 1.78 (d, *J* = 12.13 Hz, 2 H), 1.21–1.32 (m, 3 H), 1.20 (s, 3 H), and 1.18 (s, 3 H). <sup>13</sup>C NMR (151 MHz, DMSO-*d*<sub>6</sub>) δ 161.99, 159.42, 148.29, 147.84, 141.13, 131.89, 129.83, 127.98, 126.91, 126.36, 118.30, 116.32, 114.19, 47.12, 46.61, 35.19, 29.51, 28.96, 24.40, 13.87. LC-MS retention time (method 1), 2.683 min; (method 2), 3.717 min. HRMS: *m/z* (M + H)<sup>+</sup> (calculated for C<sub>25</sub>H<sub>32</sub>N<sub>5</sub> 402.2653) found, 402.2655.

*N*-(4-(1*H*-imidazol-1-yl)benzyl)-2-(2-isopropylphenyl)-5-methylpyrimidin-4-amine (**69**). 1-(4-(Chloromethyl)phenyl)-1*H*-imidazole (0.50 g, 2.60 mmol) and potassium phthalimide (0.58 g, 3.1 mmol) were heated in DMF (2.5 mL) to 120 °C for 18 h. The reaction mixture was cooled to 0 °C, poured into water, and the solids were filtered and washed with water to give 2-(4-(1*H*-imidazol-1-yl)benzyl)-isindoline-1,3-dione. The dried 2-(4-(1*H*-imidazol-1-yl)benzyl)-isindoline-1,3-dione (0.40 g, 1.32 mmol) was heated to 95 °C in a mixture of EtOH and hydrazine (4:1) for 1 h, the mixture was cooled, and the solids filtered. The solids were washed with EtOH to give (4-(1*H*-imidazol-1-yl)phenyl)methanamine. LC-MS retention time (method 1): 2.233 min. This material was used as-is in the synthesis of *N*-(4-(1*H*-imidazol-1-yl)benzyl)-2-chloro-5-methylpyrimidin-4-amine.

(4-(1*H*-Imidazol-1-yl)phenyl)methanamine 0.20 g, 1.17 mmol), 2,4-dichloro-5-methylpyrimidine (0.19 g, 1.17 mmol), and Et<sub>3</sub>N (0.33 mL, 2.34 mmol) in DMF (4 mL) were heated to 100 °C for 18 h. The reaction mixture was monitored by LC-MS; when complete, the mixture was poured into water and extracted with ethyl acetate (3×), and the organic layers were combined, dried over Na<sub>2</sub>SO<sub>4</sub>, filtered, and concentrated to give the desired intermediate. LC-MS retention time (method 1): 2.460 min. The cross coupling used the method as described in compound **48**, with a yield of 40%. <sup>1</sup>H NMR (400 MHz, DMSO-*d*<sub>6</sub>) δ 9.21 (d, *J* = 2.52 Hz, 1 H), 9.14 (s, 1 H), 8.29 (d, *J* = 1.26 Hz, 1 H), 8.07 (t, *J* = 1.64 Hz, 1 H), 7.73–7.64 (m, 3 H), 7.57–7.39 (m, 5 H), 7.33 (ddd, *J* = 1.44, 6.97, and 7.67 Hz, 1 H), 4.81 (d, *J* = 5.97 Hz, 2 H), 3.10 (td, *J* = 7.44, 13.64, and 14.23 Hz, 1 H), 2.22 (d, *J* = 1.02 Hz, 3 H), and 1.00 (d, *J* = 6.80 Hz, 6 H). <sup>13</sup>C NMR (151 MHz, DMSO-*d*<sub>6</sub>) δ 162.03, 159.83, 147.80, 142.20, 139.50, 135.11, 134.63, 131.75, 129.85, 128.75, 126.73, 126.26, 123.10, 122.07, 120.73, 118.26, 116.28, 114.36, 44.07, 29.31, 24.17, and 13.86. LC-MS retention time (method 2): 3.428 min. HRMS: *m/z* (M + H)<sup>+</sup> (calculated for C<sub>24</sub>H<sub>26</sub>N<sub>5</sub> 384.2183) found, 384.2169.

4-(1*H*-1,2,3-Triazol-1-yl)benzonitrile TFA (**x**).<sup>21</sup> 4-Aminobenzonitrile (1.00 g, 8.46 mmol) and trifluoroacetic acid (TFA) (0.65 mL, 8.46 mmol) in acetonitrile (70 mL) were stirred at room temperature for 5 min. The reaction mixture was cooled to 0 °C in a salt ice bath before the dropwise addition of *tert*-butyl nitrite (1.51 mL, 12.70 mmol), followed by azidotrimethylsilane (1.35 mL, 10.16 mmol). This reaction mixture was stirred for 30 min at 0 °C and allowed to warm to

room temperature (rt) before pouring into ethyl acetate (50 mL) and water (75 mL). The water layer was extracted (2X) with ethyl acetate, and the organic layers were combined and washed (1X) with brine. The combined organic layer was dried over  $\text{Na}_2\text{SO}_4$ , filtered, and concentrated under reduced pressure to give 1.22 g of the product as a reddish-brown solid. The compound was used as-is in the next reaction. LC-MS retention time (method 2:3 min) = 3.331 min.

4-Azidobenzonitrile (1.22 g, 8.33 mmol), sodium ascorbate (1.32 g, 6.66 mmol), copper(II) sulfate (93 mg, 0.06 mmol), and ethynyltrimethylsilane (6.20 mL, 50.0 mmol) was heated in DMSO/water (80 mL/40 mL) to 80 °C in a sealed tube for 24 h. The reaction was allowed to cool to rt, poured into ethyl acetate, and washed (3X) with 100 mL of water. The combined organic layer was dried over  $\text{Na}_2\text{SO}_4$ , filtered, and concentrated under reduced pressure to give a pale-yellow residue. The residue was taken up in acetonitrile (16 mL) and TFA (0.64 mL, 8.33 mmol) and heated to reflux for 3 h. After this time, the reaction was cooled to rt and poured in to ethyl acetate (30 mL), washed (2X) with saturated sodium bicarbonate, dried over  $\text{Na}_2\text{SO}_4$ , filtered, and concentrated and placed on a reverse phase flash system for purification (gradient 20–100% acetonitrile w/0.1% TFA in water w/0.1% TFA).  $^1\text{H}$  NMR (400 MHz,  $\text{DMSO}-d_6$ )  $\delta$  8.98 (d,  $J$  = 1.26 Hz, 1 H), and 8.22–8.00 (m, 5 H).  $^{13}\text{C}$  NMR (101 MHz,  $\text{CDCl}_3$ )  $\delta$  139.81, 135.13, 133.94, 133.14, 121.64, 120.71, 120.69, 117.68, and 112.40;  $m/z$  ( $M + \text{H}$ ) $^+$  = 171.1. LC-MS retention time (method 2:3 min): 2.671 min.

*N*-(4-(1*H*-1,2,3-Triazol-1-yl)benzyl)-2-chloro-5-methylpyrimidin-4-amine TFA (xi).<sup>21</sup> 4-(1*H*-1,2,3-Triazol-1-yl)benzonitrile (1.2 g, 7.05 mmol) and TFA (0.60 mL, 7.80 mmol) was dissolved in methanol (100 mL)/DMF (10 mL) and passed through a H-Cube Pro flow reactor using a 10% Pd/C 70 mm Catcart at 40 bar and 50 °C. Once the reaction was complete by LC-MS, the MeOH was concentrated and the crude used in the next reaction sequence. LC-MS retention time (method 2:3 min) = 1.386 min ( $m/z$  ( $M + \text{H}$ ) $^+$  = 174.2). 4-(1*H*-1,2,3-Triazol-1-yl)phenylmethanamine, TFA (7.05 mmol), 2,4-dichloro-5-methylpyrimidine (1.16 g, 7.05 mmol), and triethylamine (3.0 mL, 21.3 mmol) was heated overnight to 100 °C in DMF (25 mL). The completed reaction was poured into water (30 mL) and extracted with ethyl acetate. The ethyl acetate layer was washed (2X) with water (1X) with saturated sodium bicarbonate, dried over  $\text{Na}_2\text{SO}_4$ , filtered, and concentrated. The residue was purified on a reverse phase flash system (gradient 10–100% acetonitrile w/0.1% TFA in water w/0.1% TFA) to give 0.19 g of desired product.  $^1\text{H}$  NMR (400 MHz,  $\text{DMSO}-d_6$ )  $\delta$  8.76 (d,  $J$  = 1.17 Hz, 1 H), 7.97–7.90 (m, 2H), 7.86–7.80 (m, 3 H), 7.54–7.48 (m, 2 H), 4.63 (d,  $J$  = 5.98 Hz, 2 H), and 2.18–1.75 (m, 3 H).  $^{13}\text{C}$  NMR (101 MHz,  $\text{DMSO}-d_6$ )  $\delta$  162.60, 157.80, 154.97, 140.20, 135.90, 134.78, 129.01, 123.61, 120.61, 113.64, 43.54, and 13.50. LC-MS retention time (method 2:3 min) = 2.770 min;  $m/z$  ( $M + \text{H}$ ) $^+$  = 301.1.

*N*-(4-(1*H*-1,2,3-Triazol-1-yl)benzyl)-5-methyl-2-(2-isopropylphenyl)pyrimidin-4-amine TFA (70). *N*-(4-(1*H*-1,2,3-Triazol-1-yl)benzyl)-2-chloro-5-methylpyrimidin-4-amine (0.19 g, 0.63 mmol) was combined with (2-isopropylphenyl)boronic acid (0.31 g, 1.90 mmol), sodium carbonate (2.0 M in water, 1.23 mL, 2.53 mmol), and DPP-Pd Silicycle 0.26 mmol/g (0.30 g) in DMF (4.50 mL). The reaction was sealed and heated at 150 °C for 30 min in a Biotage Initiator microwave reactor. The resulting mixture was filtered over Celite and purified by HPLC (gradient 20–100% acetonitrile w/0.1% TFA in water w/0.1% TFA) to give, after lyophilization, *N*-(4-(1*H*-1,2,3-triazol-1-yl)benzyl)-5-methyl-2-(2-isopropylphenyl)pyrimidin-4-amine (70) as a TFA salt (0.01 g, 0.02 mmol, 30%).  $^1\text{H}$  NMR (400 MHz,  $\text{CDCl}_3$ )  $\delta$  8.82 (dd,  $J$  = 3.4, and 7.9 Hz, 1 H), 8.02–7.93 (m, 2 H), 7.76 (d,  $J$  = 1.4 Hz, 1 H), 7.64–7.56 (m, 2 H), 7.51–7.33 (m, 5 H), 7.25–7.17 (m, 1 H), 4.88 (d,  $J$  = 5.9 Hz, 2 H), 3.19 (p,  $J$  = 6.8 Hz, 1H), 2.22 (s, 3 H), 1.10 (d,  $J$  = 1.2 Hz, 3 H) and 1.09–1.07 (m, 3 H).  $^{13}\text{C}$  NMR (100 MHz,  $\text{CDCl}_3$ )  $\delta$  162.02, 160.18, 148.00, 140.63, 138.03, 136.14, 134.35, 134.28, 131.89, 130.34, 129.25, 129.00, 126.61, 126.04, 122.04, 121.99, 120.74, 113.81, 44.62, 29.43, 23.95, 13.71 and 13.67. LC-MS retention time (method 1) = 2.938 min and (method 2) = 1.756 min. HRMS: (ESI)  $m/z$  ( $M + \text{H}$ ) $^+$  (calculated for  $\text{C}_{23}\text{H}_{25}\text{N}_6$  385.2135) found, 385.2146.

*N*-(4-(1*H*-1,2,3-Triazol-1-yl)benzyl)-5-methyl-2-(2-(oxetan-3-yl)phenyl)pyrimidin-4-amine TFA (77).<sup>21</sup> 3-(2-Bromophenyl)oxetane was synthesized using the method described by Jacobsen et. al,<sup>23</sup> except diethyl 2-(2-bromophenyl)malonate was used as the starting material instead of diethyl 2-(2-(benzyloxy)phenyl)malonate. This synthetic sequence was carried out without further purification/characterization of the intermediates.

In an oven-dried 50 mL round-bottom flask, the above-mentioned 3-(2-bromophenyl)oxetane (0.14 g, 0.66 mmol) and THF (4 mL) was cooled to –78 °C. The dropwise addition of *N*-butyllithium (0.85 mL, 1.36 mmol) by syringe occurred over a 15 min period. After this time, the reaction mixture was allowed to stir at –78 °C for an additional 2 h. The contents were transferred via cannula to a second 50 mL oven-dried round-bottom flask containing a stirred solution of tripropyl borate (0.29 mL, 1.32 mmol) and THF (2.0 mL) and cooled to –78 °C. Once transferred (by cannula), the mixture was allowed to stir at –78 °C for 10 min, after which time the ice bath was removed and the reaction mixture stirred overnight. One N HCl was used to adjust the pH to ~1, and the acidic mixture was stirred for 45 min, poured into water, and extracted with diethyl ether (3X). The organic layers were combined, dried over  $\text{MgSO}_4$ , concentrated, and once the solvent was evaporated, a ~1 M solution of the crude (2-(oxetan-3-yl)phenyl)-boronic acid in 1,2-DME was made and used in next step with no further purification. In a sealed tube *N*-(4-(1*H*-1,2,3-triazol-1-yl)benzyl)-2-chloro-5-methylpyrimidin-4-amine (0.10 g, 0.33 mmol) was combined with (2-oxetainphenyl)boronic acid as a 1 M solution in DME sodium carbonate (2.0 M in water, 0.33 mL, 0.67 mmol) and DPP-Pd Silicycle 0.26 mmol/g (0.20 g) in DME (2.0 mL), and heated at 150 °C for 30 min in a Biotage Initiator microwave reactor. The resulting mixture was filtered over Celite and purified by reversed-phase HPLC (gradient 20–100% acetonitrile w/0.1% TFA in water w/0.1% TFA) to give the desired product 77.  $^1\text{H}$  NMR (400 MHz,  $\text{DMSO}-d_6$ )  $\delta$  ppm 9.36–9.47 (m, 1 H), 8.80 (s, 1 H), 8.35 (s, 1 H), 8.29 (d,  $J$  = 7.83 Hz, 1 H), 7.97 (s, 1 H), 7.90 (d,  $J$  = 8.22 Hz, 2 H), 7.68 (d,  $J$  = 8.61 Hz, 3 H), 7.52 (s, 2 H), 5.12 (br s, 1 H), 4.93–5.00 (m, 2 H), 4.41–4.50 (m, 2 H), 3.61 (dd,  $J$  = 4.30, and 10.56 Hz, 2 H), and 2.22 (s, 3 H).  $^{13}\text{C}$  NMR (151 MHz,  $\text{CDCl}_3$ )  $\delta$  161.40, 153.48, 144.27, 138.36, 137.52, 136.20, 134.57, 134.28, 129.62, 128.71, 128.52, 128.14, 126.14, 121.96, 120.88, 115.47, 109.98, 62.49, 51.61, 44.94, 39.85, and 14.15. LC-MS: method 2 (short), retention time: 2.526 min. HRMS:  $m/z$  ( $M + \text{H}$ ) (calculated for  $\text{C}_{23}\text{H}_{23}\text{N}_6\text{O}$  399.1928) found, 399.1924.

*N*-(2-(4-(1*H*-1,2,3-Triazol-1-yl)phenyl)propan-2-yl)-2-(2-isopropylphenyl)-5-methylpyrimidin-4-amine TFA (79). 2-Chloro-5-methyl-*N*-(2-(4-nitrophenyl)propan-2-yl)pyrimidin-4-amine, TFA. 2-(4-Nitrophenyl)propan-2-amine, HCl (0.60 g, 2.77 mmol), 2,4-dichloro-5-methylpyrimidine (0.45 g, 2.77 mmol), and  $\text{Et}_3\text{N}$  (1.15 mL, 8.31 mmol) in DMF (8.2 mL) was sealed and heated in a microwave vial to 150 °C for 1 h. The reaction was cooled and poured into EtOAc and washed with water (2X), dried over  $\text{Na}_2\text{SO}_4$ , filtered, and concentrated. The residue was purified using reverse phase over 30 min and gradient of 10–100 water/ $\text{CH}_3\text{CN}$  0.01% TFA to give the desired compound in a 49% yield. LC-MS retention time (method 1): 3.478 min.

2-(2-Isopropylphenyl)-5-methyl-*N*-(2-(4-nitrophenyl)propan-2-yl)pyrimidin-4-amine, TFA. 2-Chloro-5-methyl-*N*-(2-(4-nitrophenyl)propan-2-yl)pyrimidin-4-amine, TFA (0.19 g, 0.45 mmol), (2-isopropylphenyl)boronic acid (0.22 g, 1.26 mmol), sodium carbonate (2 M, 0.90 mL, 1.81 mmol), and DPP-Pd silica bound (0.20 g, 0.26 mmol/g) in dimethoxyethane (3 mL) was sealed and heated in a microwave reactor to 150 °C for 45 min. The reaction was filtered and concentrated immediately placed on a reverse phase column to give 75% of the desired intermediate, which was used without further characterization. LC-MS retention time (method 1): 3.144 min.

*N*-(2-(4-Aminophenyl)propan-2-yl)-2-(2-isopropylphenyl)-5-methylpyrimidin-4-amine. 2-(2-Isopropylphenyl)-5-methyl-*N*-(2-(4-nitrophenyl)propan-2-yl)pyrimidin-4-amine, TFA (0.28 g, 0.55 mmol), acetic acid (0.37 mL, 6.54 mmol), and zinc (0.18 g, 2.73 mmol) was stirred in  $\text{CH}_3\text{OH}$  (5.50 mL) for 1 h. The reaction mixture was filtered through a pad of Celite, rinsed with  $\text{CH}_3\text{OH}$ ,



concentrated, and used as in with no further purification or characterization. LC-MS retention time (method 1): 2.670 min. *N*-(2-(4-Aminophenyl)propan-2-yl)-2-(2-isopropylphenyl)-5-methylpyrimidin-4-amine (0.12 g, 0.33 mmol) and trifluoroacetic acid (TFA) (0.04 mL, 0.33 mmol) in acetonitrile (2 mL) was stirred at room temperature for 5 min. The reaction mixture was cooled to 0 °C in an ice bath before the dropwise addition of *tert*-butyl nitrite (0.06 mL, 0.50 mmol) followed by azidotrimethylsilane (0.05 mL, 0.40 mmol). This mixture was stirred for 30 min at 0 °C, allowed to warm to room temperature (rt), and poured into ethyl acetate (10 mL) and water (15 mL). The water layer was extracted with ethyl acetate (2×) and organic layers were combined and washed with brine (1×), dried over Na<sub>2</sub>SO<sub>4</sub>, filtered, and concentrated under reduced pressure to give to give the *N*-(2-(4-azidophenyl)propan-2-yl)-2-(2-isopropylphenyl)-5-methylpyrimidin-4-amine, which was used as-is in the next reaction without further purification. LC-MS retention time (method 1): 3.331 min. *N*-(2-(4-Azidophenyl)propan-2-yl)-2-(2-isopropylphenyl)-5-methylpyrimidin-4-amine (33 mg, 0.09 mmol), ethynyltrimethylsilane (0.13 mL, 1.03 mmol), sodium ascorbate (14 mg, 0.07 mmol), and copper(II)sulfate (1 mg, 0.006 mmol) in DMSO/H<sub>2</sub>O (1 mL/0.5 mL) was sealed in a tube and heated to 80 °C for 24 h. The cooled reaction mixture was poured into water and extracted with ethyl acetate (3×), dried over Na<sub>2</sub>SO<sub>4</sub>, filtered, concentrated, and taken up in acetonitrile (3 mL) and TFA (0.11 mL, 0.92 mmol), heated to reflux for 3 h, then the reaction was cooled and concentrated under reduced pressure. This material was purified with reverse phase to give compound **79**. <sup>1</sup>H NMR (400 MHz, DMSO-*d*<sub>6</sub>) δ 8.75 (d, *J* = 1.17 Hz, 1H), 8.23 (s, 1H), 7.94 (d, *J* = 1.13 Hz, 1H), 7.81–7.73 (m, 2H), 7.55–7.47 (m, 2H), 7.40 (t, *J* = 7.60 Hz, 1H), 7.33–7.26 (m, 1H), 7.16 (t, *J* = 7.54 Hz, 1H), 7.02 (d, *J* = 7.64 Hz, 1H), 3.05–3.17 (m, 1 H), 2.33 (d, *J* = 1.06 Hz, 3H), 1.78 (s, 6H), and 0.72 (d, *J* = 6.80 Hz, 6H). LC-MS retention time (method 2): 4.378 min. HRMS: *m/z* (M + H)<sup>+</sup>: (calculated for C<sub>25</sub>H<sub>29</sub>N<sub>6</sub> 413.2448) found, 413.2447.

**Biological Methods.** *USP1/UAF1 Quantitative High-Throughput Screening Assay.* USP1/UAF1 activity was monitored in a fluorometric ubiquitin–rhodamine110 assay as previously described.<sup>16,21</sup>

**Western Blot.** H1299 cells were seeded in 12-well plates at a density of 1 × 10<sup>5</sup> per well and allowed to attach overnight. Cells were treated with 20 μM of the indicated compounds or with an equal volume of DMSO for 4 h. Total protein extracts were prepared in RIPA lysis buffer (25 mM Tris-HCl (pH 7.6), 150 mM NaCl, 1% NP-40, 1% sodium deoxycholate, 0.1% SDS) containing protease and phosphatase inhibitor cocktail (Thermo Scientific). The concentration of protein lysates was determined using the Bio-Rad DC protein assay (Bio-Rad). Cell extracts were separated on 4–12% gradient SDS-PAGE and transferred to nitrocellulose. The membranes were blotted with PCNA antibody (PC10, Santa Cruz) or GAPDH antibody (D16H11, Cell Signaling), followed by incubation with HRP-conjugated antimouse or antirabbit secondary antibody, respectively. Blots were imaged using the Bio-Rad ChemiDoc™ XRS gel imager and quantified using ImageQuant TL (GE).

**Colony Formation Assay.** H1299 cells were seeded in 6-well plates at a density of 200 cells per well and allowed to attach overnight. Cells were treated with 5 μM of the indicated compounds or with an equal volume of DMSO. Seven days after compound treatment, plates were fixed with 20% methanol and stained with 0.1% crystal violet. Plates were imaged with the Typhoon FLA 7000 (GE), and colonies were counted using ImageQuant TL (GE). Cell survival was expressed in percentage with DMSO-treated cells set as 100%.

## ■ ASSOCIATED CONTENT

### ■ Supporting Information

Additional supplemental figures, experimental procedures, and spectroscopic data (<sup>1</sup>H NMR, LC-MS and HRMS) for representative compounds. This material is available free of charge via the Internet at <http://pubs.acs.org>.

## ■ AUTHOR INFORMATION

### Corresponding Authors

\*For D.J.M.: phone, 301-217-4381; fax, 301-217-5736; E-mail, [maloneyd@mail.nih.gov](mailto:maloneyd@mail.nih.gov).

\*For Z.Z.: phone, 302-831-8940; E-mail, [zzhuang@udel.edu](mailto:zzhuang@udel.edu).

### Author Contributions

<sup>§</sup>These authors (T.S.D. and A.S.R.) contributed equally to this work.

### Notes

The authors declare no competing financial interest.

## ■ ACKNOWLEDGMENTS

This work was supported in part by U.S. National Institutes of Health (NIH) grants R03DA030552 and R01GM097468 to Z.Z. T.S.D., A.S.R., D.K.L., E.H.K., A.S., A.J., and D.J.M. were supported by the intramural research program of the National Center for Advancing Translational Sciences and the Molecular Libraries Initiative of the National Institutes of Health Roadmap for Medical Research (U54MH084681). We thank Sam Michael and Richard Jones for automation support, Paul Shinn Misha Itkin, and Danielle van Leer for the assistance with compound management, William Leister, Heather Baker, Elizabeth Fernandez, and Christopher Leclair for analytical chemistry and purification support, and Kimloan Nguyen for in vitro ADME data.

## ■ ABBREVIATIONS USED

DUBs, deubiquitinases; USP1, ubiquitin-specific protease 1; UAF1, USP1-associated factor 1; PCNA, proliferating cell nuclear antigen; FANCD2, Fanconi anemia group complementation group D2; IS, inhibitor of DNA binding; HTS, high-throughput screening; ADME, absorption, distribution, metabolism, elimination; POCl<sub>3</sub>, phosphorus oxychloride; HOBT, hydroxybenzotriazole; DMF, dimethylformamide; DME, dimethoxyethane; DPP, diphenylphosphine; MW, microwave; DCE, dichloroethane; DMSO, dimethyl sulfoxide; LAD, lithium aluminum deuteride; TFA, trifluoroacetic acid; SAR, structure–activity relationship; qHTS, quantitative high-throughput screening; CYP, cytochrome P450; Ub-Rho, ubiquitin rhodamine; NADPH, nicotinamide adenine dinucleotide phosphate; GAPDH, glyceraldehyde 3-phosphate dehydrogenase; RLM, rat liver microsome; MLM, mouse liver microsome; HLM, human liver microsome; CFA, colony formation assay

## ■ REFERENCES

- (1) Pickart, C. M. Mechanisms underlying ubiquitination. *Annu. Rev. Biochem.* **2001**, 70, 503–533.
- (2) Komander, D.; Rape, M. The ubiquitin code. *Annu. Rev. Biochem.* **2012**, 81, 203–229.
- (3) Bergink, S.; Jentsch, S. Principles of ubiquitin and SUMO modifications in DNA repair. *Nature* **2009**, 458, 461–467.
- (4) Conaway, R. C.; Brower, C. S.; Conaway, J. W. Emerging roles of ubiquitin in transcription regulation. *Science* **2002**, 296, 1254–1258.
- (5) Mukhopadhyay, D.; Riezman, H. Proteasome-independent functions of ubiquitin in endocytosis and signaling. *Science* **2007**, 315, 201–205.
- (6) Nakayama, K. I.; Nakayama, K. Ubiquitin ligases: cell-cycle control and cancer. *Nature Rev. Cancer* **2006**, 6, 369–381.
- (7) Komander, D.; Clague, M. J.; Urbe, S. Breaking the chains: structure and function of the deubiquitinases. *Nature Rev. Mol. Cell Biol.* **2009**, 10, 550–563.

- (8) Rentsch, A.; Landsberg, D.; Brodmann, T.; Bulow, L.; Girbig, A. K.; Kalesse, M. Synthesis and pharmacology of proteasome inhibitors. *Angew. Chem., Int. Ed.* **2013**, *52*, 5450–5488.
- (9) Bedford, L.; Lowe, J.; Dick, L. R.; Mayer, R. J.; Brownell, J. E. Ubiquitin-like protein conjugation and the ubiquitin–proteasome system as drug targets. *Nature Rev. Drug Discovery* **2011**, *10*, 29–46.
- (10) Cohn, M. A.; Kowal, P.; Yang, K.; Haas, W.; Huang, T. T.; Gygi, S. P.; D'Andrea, A. D. A UAF1-containing multisubunit protein complex regulates the Fanconi anemia pathway. *Mol. Cell* **2007**, *28*, 786–797.
- (11) Huang, T. T.; Nijman, S. M.; Mirchandani, K. D.; Galaray, P. J.; Cohn, M. A.; Haas, W.; Gygi, S. P.; Ploegh, H. L.; Bernards, R.; D'Andrea, A. D. Regulation of monoubiquitinated PCNA by DUB autocleavage. *Nature Cell Biol.* **2006**, *8*, 339–347.
- (12) Nijman, S. M.; Huang, T. T.; Dirac, A. M.; Brummelkamp, T. R.; Kerkhoven, R. M.; D'Andrea, A. D.; Bernards, R. The deubiquitinating enzyme USP1 regulates the Fanconi anemia pathway. *Mol. Cell* **2005**, *17*, 331–339.
- (13) Williams, S. A.; Maecker, H. L.; French, D. M.; Liu, J.; Gregg, A.; Silverstein, L. B.; Cao, T. C.; Carano, R. A.; Dixit, V. M. USP1 deubiquitinates ID proteins to preserve a mesenchymal stem cell program in osteosarcoma. *Cell* **2011**, *146*, 918–930.
- (14) Lasorella, A.; Benezra, R.; Iavarone, A. The ID proteins: master regulators of cancer stem cells and tumour aggressiveness. *Nature Rev. Cancer* **2014**, *14*, 77–91.
- (15) Garcia-Santisteban, I.; Peters, G. J.; Giovannetti, E.; Rodriguez, J. A. USP1 deubiquitinase: cellular functions, regulatory mechanisms and emerging potential as target in cancer therapy. *Mol. Cancer* **2013**, *12*, 91.
- (16) Chen, J.; Dexheimer, T. S.; Ai, Y.; Liang, Q.; Villamil, M. A.; Inglese, J.; Maloney, D. J.; Jadhav, A.; Simeonov, A.; Zhuang, Z. Selective and Cell-Active Inhibitors of the USP1/ UAF1 Deubiquitinase Complex Reverse Cisplatin Resistance in Non-small Cell Lung Cancer Cells. *Chem. Biol.* **2011**, *18*, 1390–1400.
- (17) Brown, P. J.; Stuart, L. W.; Hurley, K. P.; Lewis, M. C.; Winegar, D. A.; Wilson, J. G.; Wilkison, W. O.; Ittoop, O. R.; Willson, T. M. Identification of a subtype selective human PPAR $\alpha$  agonist through parallel-array synthesis. *Bioorg. Med. Chem. Lett.* **2001**, *11*, 1225–1227.
- (18) Nelson, E. A.; Walker, S. R.; Weisberg, E.; Bar-Natan, M.; Barrett, R.; Gashin, L. B.; Terrell, S.; Klitgaard, J. L.; Santo, L.; Addorio, M. R.; Ebert, B. L.; Griffin, J. D.; Frank, D. A. The STAT5 inhibitor pimozone decreases survival of chronic myelogenous leukemia cells resistant to kinase inhibitors. *Blood* **2011**, *117*, 3421–3429.
- (19) Roth, B. L.; Craigo, S. C.; Choudhary, M. S.; Uluer, A.; Monsma, F. J., Jr.; Shen, Y.; Meltzer, H. Y.; Sibley, D. R. Binding of typical and atypical antipsychotic agents to 5-hydroxytryptamine-6 and 5-hydroxytryptamine-7 receptors. *J. Pharmacol. Exp. Ther.* **1994**, *268*, 1403–1410.
- (20) Mistry, H.; Hsieh, G.; Buhrlage, S. J.; Huang, M.; Park, E.; Cuny, G. D.; Galinsky, I.; Stone, R. M.; Gray, N. S.; D'Andrea, A. D.; Parmar, K. Small-molecule inhibitors of USP1 target ID1 degradation in leukemic cells. *Mol. Cancer Ther.* **2013**, *12*, 2651–2662.
- (21) Liang, Q.; Dexheimer, T. S.; Zhang, P.; Rosenthal, A. S.; Villamil, M. A.; You, C.; Zhang, Q.; Chen, J.; Ott, C. A.; Sun, H.; Luci, D. K.; Yuan, B.; Simeonov, A.; Jadhav, A.; Xiao, H.; Wang, Y.; Maloney, D. J.; Zhuang, Z. A selective USP1-UAF1 inhibitor links deubiquitination to DNA damage responses. *Nature Chem. Biol.* **2014**, *10*, 298–304.
- (22) Purandare, A. V.; Gao, A.; Wan, H.; Somerville, J.; Burke, C.; Seachord, C.; Vaccaro, W.; Wityak, J.; Poss, M. A. Identification of chemokine receptor CCR4 antagonist. *Bioorg. Med. Chem. Lett.* **2005**, *15*, 2669–2672.
- (23) Dehnhardt, C. M.; Venkatesan, A. M.; Chen, Z.; Ayril-Kaloustian, S.; Dos Santos, O.; de los Santos, E.; Curran, K.; Follettie, M. T.; Diesl, V.; Lucas, J.; Geng, Y.; Dejoy, S. Q.; Petersen, R.; Chaudhary, I.; Brooijmans, N.; Mansour, T. S.; Arndt, K.; Chen, L. Design and synthesis of novel diaminoquinazolines with in vivo efficacy for beta-catenin/T-cell transcriptional factor 4 pathway inhibition. *J. Med. Chem.* **2010**, *53*, 897–910.
- (24) Surry, D. S.; Buchwald, S. L. Dialkylbiaryl Phosphines in Pd-Catalyzed Amination: A User's Guide. *Chem. Sci.* **2011**, *2*, 27–50.
- (25) Surry, D. S.; Buchwald, S. L. Biaryl phosphane ligands in palladium-catalyzed amination. *Angew. Chem., Int. Ed.* **2008**, *47*, 6338–6361.
- (26) Barral, K.; Moorhouse, A. D.; Moses, J. E. Efficient conversion of aromatic amines into azides: a one-pot synthesis of triazole linkages. *Org. Lett.* **2007**, *9*, 1809–1811.
- (27) Kim, J. M.; Cho, I. S.; Mariano, P. S. Amine-flavin electron transfer photochemistry. Potential models for monoamine oxidase catalysis and inhibition. *J. Org. Chem.* **1991**, *56*, 4943–4955.
- (28) Loy, R. N.; Jacobsen, E. N. Enantioselective intramolecular openings of oxetanes catalyzed by (salen)Co(III) complexes: access to enantioenriched tetrahydrofurans. *J. Am. Chem. Soc.* **2009**, *131*, 2786–2787.
- (29) Gant, T. G. Using deuterium in drug discovery: leaving the label in the drug. *J. Med. Chem.* **2014**, *57*, 3595–3611.
- (30) Foster, A. B. Deuterium isotope effects in the metabolism of drugs and xenobiotics: Implications for drug design. *Adv. Drug Res.* **1985**, *14*, 1–40.
- (31) Cohen, P.; Tcherpakov, M. Will the ubiquitin system furnish as many drug targets as protein kinases? *Cell* **2010**, *143*, 686–693.
- (32) Murai, J.; Yang, K.; Dejsuphong, D.; Hirota, K.; Takeda, S.; D'Andrea, A. D. The USP1/UAF1 complex promotes double-strand break repair through homologous recombination. *Mol. Cell. Biol.* **2011**, *31*, 2462–2469.
- (33) Lim, K. H.; Baek, K. H. Deubiquitinating enzymes as therapeutic targets in cancer. *Curr. Pharm. Des.* **2013**, *19*, 4039–4052.
- (34) Hussain, S.; Zhang, Y.; Galaray, P. J. DUBs and cancer: the role of deubiquitinating enzymes as oncogenes, non-oncogenes and tumor suppressors. *Cell Cycle* **2009**, *8*, 1688–1697.
- (35) Yang, J. M. Emerging roles of deubiquitinating enzymes in human cancer. *Acta Pharmacol. Sin.* **2007**, *28*, 1325–1330.